Atmos. Chem. Phys. Discuss., 15, 15469–15510, 2015
www.atmos-chem-phys-discuss.net/15/15469/2015/
doi:10.5194/acpd-15-15469-2015

Atmospheric Chemistry and Physics Discussions

Chemical and physical influences on aerosol activation in liquid clouds: an empirical study based on observations from the Jungfraujoch, Switzerland

C. R. Hoyle[1,2], C. S. Webster[1,2], H. E. Rieder[3,4], E. Hammer[1,*], M. Gysel[1], N. Bukowiecki[1], E. Weingartner[1], M. Steinbacher[5], and U. Baltensperger[1]

[1]Laboratory of Atmospheric Chemistry, Paul Scherrer Institute, Villigen, Switzerland
[2]Swiss Federal Institute for Forest Snow and Landscape Research (WSL)-Institute for Snow and Avalanche Research (SLF), Davos, Switzerland
[3]Wegener Center for Climate and Global Change and IGAM/Department of Physics University of Graz, Austria
[4]Austrian Polar Research Institute, Vienna, Austria
[5]Laboratory for Air Pollution/Environmental Technology, Empa – Swiss Federal Laboratories for Materials Science and Technology, Ueberlandstrasse 129,8600 Duebendorf, Switzerland
[*]now at: Grolimund + Partner – Environmental Engineering, Thunstrasse 101a, 3006 Bern, Switzerland

Received: 1 May 2015 – Accepted: 19 May 2015 – Published: 9 June 2015

Correspondence to: C. R. Hoyle (christopher.hoyle@psi.ch)

Published by Copernicus Publications on behalf of the European Geosciences Union.

ACPD
15, 15469–15510, 2015

Abstract

A simple empirical model to predict the number of aerosols which activate to form cloud droplets in a warm, free tropospheric cloud has been established, based on data from four summertime Cloud and Aerosol Characterisation Experiments (CLACE) campaigns at the Jungfraujoch (JFJ). It is shown that 76 % of the observed variance in droplet numbers can be represented by a model accounting only for the number of potential CCN (defined as number of particles larger than 90 nm in diameter), while the mean errors in the model representation may be reduced by the addition of further explanatory variables, such as the mixing ratios of O_3, CO and the height of the measurements above cloud base. The model has similar ability to represent the observed droplet numbers in each of the individual years, as well as for the two predominant local wind directions at the JFJ (north west and south east). Given the central European location of the JFJ, with air masses in summer being representative of the free troposphere with regular boundary layer in-mixing via convection, we expect that this model is applicable to warm, free tropospheric clouds over the European continent.

1 Introduction

Aerosols have a well-documented and pronounced influence on the microphysical and therefore radiative properties of warm clouds (e.g., Twomey, 1974, 1977; Albrecht, 1989; Hu and Stamnes, 1993). The properties of atmospheric aerosol particles thus have a strong potential to affect local and regional climates. However, the influence of aerosols on clouds remains the single largest uncertainty hampering the calculation of future climate scenarios (Boucher et al., 2013). In order to reduce this uncertainty, an improved understanding of the aerosol properties and environmental conditions that allow parts of the aerosol population to act as cloud condensation nuclei (CCN) and form cloud droplets is required.

ACPD
15, 15469–15510, 2015

It has long been recognised that the number and the size of aerosol particles strongly influences the number of CCN, and that at higher aerosol number concentrations, clouds will be composed of a greater number of droplets (Köhler, 1936; Fitzgerald and Spyers-Duran, 1973; Twomey, 1974, 1977). Several simple parametrisations of the number of cloud droplets as a function of the aerosol diameter and total aerosol number have been put forward for both continental and maritime locations, (Köhler, 1936; Raga and Jonas, 1993; Jones, 1994; Martin et al., 1994), mainly for stratus and stratocumulus clouds.

Subsequently, more advanced parametrisations were developed, allowing for the influence of the aerosol size distribution, updraught velocity, and the chemical composition and mixing state of the aerosol to be accounted for when calculating aerosol water uptake and activation to form cloud droplets (e.g., Barahona and Nenes, 2007; Fountoukis and Nenes, 2005; Kumar et al., 2009; Nenes and Seinfeld, 2003; Petters and Kreidenweis, 2007).

Previous ground-based studies have investigated statistical relationships between CCN concentration, aerosol properties and environmental variables (e.g., Henning et al., 2002; Dusek et al., 2006; Verheggen et al., 2007; Jurányi et al., 2010, 2011; Anttila et al., 2012). Based on around 22 days of data from the Taunus Observatory in central Germany, Dusek et al. (2006) determined that the concentration of CCN (as measured at different supersaturations in a CCN counter) is largely dependent on the measured particle size distribution, with the CCN concentration increasing with increasing particle diameter, and chemical composition of the aerosol playing a secondary role. Examining one month of data from a remote site in northern Finland, Anttila et al. (2012) determined that the highest correlations with activated aerosol number occur with the number of available CCN, which was defined as the total number of particles greater than 100 nm in diameter, and that the number of droplets formed did not strongly depend on updraught velocity.

A set of regimes where the number of cloud droplets formed depends on updraught velocities (at low ratios of updraught to aerosol number), and where the number of

ACPD
15, 15469–15510, 2015

cloud droplets depends more on the number of aerosol (at high ratios of updraught to aerosol number) were described by Reutter et al. (2009), based on cloud parcel model studies. At the Jungfraujoch site, Henning et al. (2002) determined that in clouds with liquid water contents above 0.15 g m^{-3}, aerosol larger than 100 nm in diameter was typically activated to form cloud droplets. Verheggen et al. (2007) investigated relationships between environmental variables and activated fraction, defined as the fraction of total particles, larger than 100 nm in diameter, that have been activated to form cloud droplets. The latter study based its analysis on one summer and two winter campaigns, and found that the activated fraction increased with increasing liquid water content and decreased with decreasing temperature below 0 °C, as clouds began to glaciate. Also using data from the Jungfraujoch site, Jurányi et al. (2010, 2011) found that with knowledge of the average chemical composition of aerosol, a very high degree of correlation could be found between the number of activated aerosol predicted by the κ-Köhler approach (Petters and Kreidenweis, 2007) and the observed number of activated particles measured at different supersaturations in a CCN counter.

Various studies have investigated the way in which the chemical composition of aerosol influences its water uptake and activation, and how this can be accounted for (e.g. Köhler, 1936; McFiggans et al., 2006; Petters and Kreidenweis, 2007). In addition, surface active compounds may influence the surface tension of aerosol droplets and thus activation to form droplets (Shulman et al., 1996; Shilling et al., 2007; King et al., 2009). Recently, it has been suggested that this may lead to a temperature influence on aerosol activation (Christensen and Petters, 2012). Nevertheless, the works of, for example, Dusek et al. (2006); Jurányi et al. (2010, 2011) suggest that the relatively small variations in chemical composition of aerosol in areas away from sources may play a smaller role in determining CCN activity of the aerosol than variations in the size distribution.

Although both Dusek et al. (2006) and Jurányi et al. (2010, 2011) have found that with a known aerosol size distribution, one can obtain good correlations between the predicted and observed number of droplets at a particular supersaturation in a CCN

ACPD
15, 15469–15510, 2015

counter, the peak supersaturation reached in an air parcel is not generally a known quantity. It is also not possible to say how well the number of droplets predicted in this way corresponds with the number of droplets in a cloud which has formed some time ago. A simple method of predicting cloud droplet numbers based on more easily quantifiable parameters would therefore be useful.

In this study, data from four summer measurement campaigns carried out at the Jungfraujoch between 2002 and 2011 are used to develop simple statistical models of the relationship between the number of observed cloud droplets and various environmental factors, as well as the aerosol number size distribution. Using such an extensive data set collected over a period of nearly ten years allows the construction of relationships which are applicable to a wide range of conditions.

2 Measurement site

The Jungfraujoch (JFJ) high alpine measurement site is located at 3580 m a.s.l., below an exposed crest in the Bernese Alps, Switzerland, and is accessible by train throughout the year. The site is engulfed in cloud approximately 40 % of the time (Baltensperger et al., 1998; Nyeki et al., 1998) and local emissions are minimal with the exception of occasional construction activities. Aerosol measurements have been carried out at the JFJ since 1988 (Baltensperger et al., 1991, 1997) and the site has been part of the Global Atmosphere Watch (GAW) programme since 1995. The location of the station makes it suitable for continuous monitoring of the free troposphere. The topography around the measurement site defines two predominant local wind directions, southeast or northwest. To the southeast, the Aletsch Glacier gradually slopes away from the JFJ at an approximate angle of 15°. In contrast, the northwestern side drops steeply at an average slope of approximately 46°. This difference in topography causes updraught velocities to be higher in air masses approaching the station from the northwest than from the southeast, with median peak supersaturations of around 0.41 % (represen-

ACPD
15, 15469–15510, 2015

tative of cumulus clouds) and 0.22 % (representative of shallow layer clouds) being reached for the respective wind directions (Hammer et al., 2014a).

The unique topography surrounding the JFJ site and the long-term measurements performed there provide substantial opportunity for not only investigating how relationships between environmental variables change between years, but also what effect the differing topography to the north and south has, through its influence on the vertical wind velocity. Furthermore, the composition of aerosols in air coming from the south will be influenced by different source regions than air coming from the north. Peak supersaturation values, updraught velocity, aerosol hygroscopicity and cloud droplet number concentration were studied by Hammer et al. (2014a), who found that all these quantities showed statistically significant differences between the two wind sectors. This work was extended by Hammer et al. (2014b), who quantified the influence of updraught velocity and particle composition and concentration on peak supersaturation.

While measurements made at the station mostly sample the free troposphere, in summer the air masses are regularly influenced by injections of boundary layer air, due to convective events (Lugauer et al., 1998; Nyeki et al., 1998) and frontal systems (Zellweger et al., 2003).

The JFJ observatory is also one of 16 stations of the Swiss National Air Pollution Monitoring Network. As part of this operation, continuous in-situ observations of about 70 different trace gases are performed by Empa, the Swiss Federal Laboratories for Materials Science and Technology.

3 Data collection

Data used in this study were collected as part of the Cloud and Aerosol Characterisation Experiments (CLACE). The CLACE experiments have been conducted at the JFJ since 2000. They are a series of intensive winter and summer campaigns designed to investigate the chemical, physical and optical properties of aerosols as well as their interaction with clouds (Henning et al., 2002; Verheggen et al., 2007; Sjogren

ACPD
15, 15469–15510, 2015

et al., 2008; Kammermann et al., 2010; Jurányi et al., 2010, 2011; Hammer et al., 2014a). The present study utilises data collected during four summer campaigns, in 2002, 2004, 2010, and 2011 (Table 1).

The following description refers to the basic experimental setup during all CLACE campaigns. The particles and hydrometeors were sampled via a total and an interstitial inlet which were installed through the roof of the laboratory (Hammer et al., 2014a). The total inlet sampled all the particles that had a diameter of less than 40 µm, including the hydrometeors, at wind speeds up to 20 m s^{-1} (Weingartner et al., 1999). The condensed water of the particles and hydrometeors was evaporated by heating up the top part of the inlet to approximately 25 °C so that all particles were dried (and therefore residual aerosol contained in cloud droplets was set free) while reaching the instruments in the laboratory. The interstitial inlet only sampled particles smaller than 1 and 2 µm diameter using a size discriminator of PM_1 (during CLACE2002) and PM_2 (during CLACE2004, CLACE2010 and CLACE2011) respectively. Thus, only non-activated particles (i.e. particles that did not act as CCN, and were thus not contained in cloud droplets) passed this inlet. The transition to laboratory temperatures (typically 20 to 30 °C) resulted in the drying of the particles at a relative humidity less than 10 %. The difference between the number of aerosol sampled through the total inlet and the number sampled through the interstitial inlet gives the number of aerosol which were activated to form cloud droplets, n_{act}. It has been shown by Henning et al. (2002), in a comparison with Forward Scattering Spectrometer Probe (FSSP) droplet measurements, that this value can be used as a proxy for the number of cloud droplets. Therefore this is the approach that we adopt in the present study.

Downstream of the inlets, a Scanning Mobility Particle Sizer (SMPS) was used to measure the total and interstitial aerosol size distribution, respectively. The SMPS instrument measured particles in the size range of 16 to 600 nm. One scan required 6 min. During CLACE2002 and CLACE2004, the SMPS was installed behind a pinch valve to switch between the two inlets after each scan (i.e. 6 min). The data in 2002 and 2004 is therefore at 12 min resolution. For CLACE2010 and CLACE2011, two SMPS

ACPD
15, 15469–15510, 2015

measured simultaneously behind each inlet so that a higher time resolution (approximately 6 min) could be achieved. Each SMPS consists of a differential mobility analyser (DMA), a bipolar charger to obtain charge equilibrium (krypton source, ^{85}Kr) and a condensation particle counter (CPC) (Wiedensohler et al., 2012). During cloud-free periods, the interstitial and the total SMPS should measure the same aerosol number size distribution. For the campaigns where two SMPS measured simultaneously, the out-of-cloud particle size distribution showed differences of up to 10 % for particles with diameters between 20 and 600 nm (Hammer et al., 2014a). This is within the typical uncertainty for this type of measurements (Wiedensohler et al., 2012). To account for these differences between the two units, the interstitial number size distributions (for each campaign specific instrument) were corrected towards the total aerosol size distribution. A size and time dependent correction factor was determined by comparing the total and interstitial number size distributions during all cloud-free periods (Verheggen et al., 2007).

To monitor the cloud presence, the liquid water content (LWC) was measured using a particle volume monitor (PVM-100; Gerber, 1991), which measures the LWC by forward light scattering.

A measurement of the horizontal wind speed and direction was provided by the Rosemount Pitot tube anemometer, which is mounted on a 10 m mast as part of the SwissMetNet network of MeteoSwiss. Likewise, temperature measured at the site as part of the SwissMetNet network was used.

In recent years, outdoor tourism activities around the JFJ have increased, resulting in more frequent local pollution events. Data that is likely affected by construction activities, snow groomer operation and other local anthropogenic influences have been removed from the data sets.

In-situ trace gas measurements of O_3 and CO were conducted as part of the Swiss National Air Pollution Monitoring Network. Measurements were recorded at 10 min intervals throughout all study periods, using a UV absorption technique for O_3 (Thermo Environmental Instrument, TEI49C), and non-dispersive IR absorption photometry

ACPD
15, 15469–15510, 2015

(NDIR) for CO (Horiba APMA360, APMA370) (Gilge et al., 2010; Zellweger et al., 2009).

4 Data analysis

4.1 Data processing

For years where two SMPS were operating simultaneously (CLACE2010, CLACE2011), n_{act}, as a function of dry particle diameter, could be calculated directly from the difference between the total and the interstitial particle number size distributions. For the remaining two years (CLACE2002 and CLACE2004), the SMPS was switched between the total and the interstitial inlet, the total measurement was assumed to be the first measurement, with the interstitial measurement immediately following used to calculate n_{act}. The two scans inside this 12 min period were assumed to represent the same conditions.

In order to exclude cloud periods that were influenced by the entrainment of dry air, as well as to exclude mixed phase clouds, the fraction of activated particles was analysed as a function of particle diameter. Without entrainment, all particles above a particular size will be activated. This size, the activation diameter, corresponds to the critical diameter of the least hygroscopic particle, at the highest supersaturation encountered during the cloud formation. As described below, for the aged aerosol found at the JFJ, the critical diameter lies around 90–100 nm. Entrainment and mixing of air into the cloud will lead to non-activated particles larger than the activation diameter co-existing with activated particles and therefore the maximum activated fraction above the activation diameter will be less than one. Similarly, the lower water vapour pressure over ice particles in mixed phase clouds will lead to evaporation of droplets and deactivation of aerosol, reducing the activated fraction above the activation diameter. A threshold of 0.9 was defined, and all measurements with maximum activated

ACPD
15, 15469–15510, 2015

fractions of less than this threshold were assumed to be influenced by entrainment or partial glaciation of the cloud and thus excluded from the analysis.

The data were also filtered to remove any data points that were measured outside of clouds, in patchy cloud, or on the edges of clouds. This was achieved based on the measured LWC. For the campaigns that had two SMPS scanners operating simultaneously (CLACE2010 and CLACE2011), the criterion follows Hammer et al. (2014a), where cloud was defined to be present when the 30th-percentile of the 10 s LWC values' distribution during one 6 min scan period was higher than 5 mg m^{-3}. For the other campaigns which had only one SMPS system operating (CLACE2002 and CLACE2004), creating a 12 min resolution data set, the criterion used was that of Henning et al. (2002) and Cozic et al. (2008), which defined cloudy conditions if the LWC was higher than 20 mg m^{-3} for more than 85 % of an hourly period.

Total water content (TWC) was calculated by adding measured LWC to calculated gas phase water (GPW), except during CLACE2010 where it could be determined directly from a dew point measurement in air sampled through the total inlet. In campaigns other than CLACE2010, such dew point measurements were not available and the GPW was calculated, using the ambient temperature, under the assumption that the in-cloud relative humidity was 100 %.

Data was classified according to wind direction (north and south), in order to determine if different factors influence the CCN quality depending on the origin of the aerosol particles.

For the purposes of this study, an estimate of the updraught velocity (w_{act}) at cloud base was calculated, similarly to Hammer et al. (2014a), from the local topography and the horizontal wind speed measured at the JFJ (v^{h}_{JFJ}) using:

$$w_{act} = \tan(\alpha) v^{h}_{JFJ}, \quad (1)$$

where α is the inclination angle of the flow lines at the cloud base. These values were $\alpha = 46^{\circ}$ for the northern terrain and $\alpha = 15^{\circ}$ for the southern terrain (for further details see Hammer et al., 2014a). This equation is based on the assumptions that the flow

ACPD
15, 15469–15510, 2015

lines of the updraught strictly follow the terrain on either side of the JFJ research station, and that there is neither sideways convergence nor divergence of the flow lines between the cloud base and the JFJ.

The dry activation diameter of the aerosol was calculated for each measurement time, following Hammer et al. (2014a). As the activation diameter is not sharply defined, rather the proportion of activated particles increases between approximately 0 and 1 over a small range of diameters, the activation diameter is defined as that at which half the particles are activated and half are unactivated.

4.2 Selection of predictor variables

Six different predictor variables either measured at the JFJ, or calculated for the cloud base, were included in the statistical analysis. These were height of the JFJ above cloud base, updraught velocity, number of available potential CCN particles (hereafter referred to as n_{CCN}, see definition below), air temperature at the cloud base, CO and O_3.

The height of the JFJ above the cloud base (calculated from the total water content and temperature measured at the JFJ) was included as it determines the amount of condensed water at the altitude of the measurements, and it is also related to the age of the cloud, during which scavenging or coagulation processes may occur.

The updraught velocity, estimated as described in Sect. 4.1, was chosen as it is known to influence the peak supersaturation achieved during cloud formation, and therefore the activation diameter of the aerosol and the activated fraction of a particular aerosol size distribution.

The n_{CCN} is estimated from the measured aerosol size distributions. As described in Sect. 1, the aerosol number size distribution is known to play an important role in defining the number of cloud droplets formed, with larger particles more likely to be activated, and the smallest particles rarely playing a role in cloud formation. Therefore, it is necessary to choose a minimum diameter, above which a particle can be considered a potential CCN. As described above, at aerosol number concentrations larger than

ACPD
15, 15469–15510, 2015

approximately 100 cm^{-3}, Henning et al. (2002) found that the activation diameter at the JFJ is around 100 nm. Further, Hammer et al. (2014a) reported that there is a systematic difference in the activation diameter for aerosol in air masses approaching the JFJ from the north (87 nm) and from the south (106 nm). Here we have chosen 90 nm. The relatively low value was chosen so as not to exclude potentially important sizes of aerosols.

The air temperature at cloud base (calculated from the temperature at the JFJ) was chosen to account for any temperature dependent effects on water uptake to the aerosols which may influence activation, however the cloud base temperature was found not to contribute significantly in the linear regression models for the years 2010 and 2011 (i.e., the years with most observational data) and was thus excluded by backward-elimination of explanatory variables for final model selection. Likewise, no significant relationship between air pressure and n_{act} was found.

Finally, the two chemical tracers CO and O_3 were included in the analysis to account for the history of the air parcels. While CO is a primary pollutant and O_3 is produced photochemically as a secondary pollutant from precursors such as volatile organic compounds and nitrogen oxides, both of these can act as tracers of anthropogenic emissions or of biomass burning events (e.g. Staudt et al., 2001; Liang et al., 2004; Yashiro et al., 2009; Zhang et al., 2006, 2009; Gilge et al., 2010), and therefore in this study they are used as indicators of the degree of influence of polluted air masses, in an attempt to determine if this has an important effect on particle activation at the JFJ. Ozone at the JFJ may be influenced by stratospheric intrusions, however a recent modelling study (Cui et al., 2009) has suggested that this is the case for less than 20 % of the year, making such events relatively rare.

4.3 Statistical analysis

In order to determine if and how environmental and chemical factors can be related to the number of cloud droplets (i.e. the number of activated aerosol, n_{act}), we chose

ACPD
15, 15469–15510, 2015

a simple multiple linear regression model for the analysis. Multiple linear regression is a commonly used statistical method for explanatory and theory-testing purposes, thus it is appropriate to use in assessing how the environmental and chemical variables contribute to the prediction of n_{act} (Johnson et al., 2004; Tonidandel and LeBreton, 2011). It is likely that several of the predictor variables selected for this analysis will be cross-correlated, thus traditional regression indices (p value, regression coefficients) will fail to appropriately partition the predictor variables into respective contribution to the overall R^2 of the model (Tonidandel and LeBreton, 2011). Nevertheless, active research in the statistical sciences has led to a set of tools for the assessment of the relative importance of individual covariates in linear regression models in the presence of correlated explanatory variables. A widely used approach, first proposed by Lindeman and Gold (1980), hence referred to as LMG, but better known in the sequential additive version proposed by Kruskal (1987), allows assigning shares of "relative importance" to a set of regressors in a linear model (Grömping, 2007). Here we use the LMG method, in its implementation in the *relaimpo* package, developed by Grömping (2006) available for the scientific computing language R (R Core Team, 2014), to assess the relative importance of individual explanatory variables in a simple linear regression model for the cloud droplet numbers in warm, free tropospheric clouds.

In the following we propose simple linear regression models developed based on 4 years of observations from the JFJ, Switzerland. Additionally the regression model was run for subsets of the data corresponding to the different years, and wind directions to investigate its general applicability.

The aim of this analysis was to determine whether a single statistical model can be constructed which will be generally applicable for the prediction of the number of cloud droplets for all years and wind directions.

ACPD
15, 15469–15510, 2015

5 Results

In total, 2399 data points were included in the analysis, with the majority being from 2010 (1087) and 2011 (896). Data was limited in 2002 (206 points) and 2004 (210 points) compared to that in 2010 and 2011 since there were more episodes of entrainment or partially glaciated clouds, where data was excluded from this analysis. Additionally, the time resolution of the measurement data set was lower in 2004 and 2002 than in later years, as described above, yielding fewer data points. In Figs. 1 to 4, time series of the predictor variables are shown for each campaign. In these plots, it can be seen that the data sets include a wide range of conditions with respect to meteorology and air parcel composition. In the upper panels of the plots, n_{CCN} is plotted together with n_{act}. In 2011 and 2010 (Figs. 1 and 2) there are episodes of relatively high n_{CCN}, during which activation of CCN larger than 90 nm is not complete, as shown by the lower n_{act} numbers. Additionally, activation appears to be lower when the wind is from the southeast (red symbols in the bottom panel of the plots). In 2004 however (Fig. 3), n_{CCN} is generally fairly low, with, in a few cases, larger n_{act} than CCN, indicating that also particles below the chosen cut off diameter for potential CCN are being activated. In 2002 (Fig. 4), there is a broad range of n_{CCN} values, and activation appears to be high in almost all cases, regardless of wind direction or updraught velocity. In all years, the concentrations of CO and O_3 (second panel) appear to be fairly well correlated, except around day 12 of the 2002 campaign (overall $R = 0.65$). There does not appear to be an appreciable link between wind direction and CO or O_3 concentration. The temperature range is similar for all the data sets, with temperatures generally between 270 and 280 K. An episode of warmer temperatures in the first half of the 2010 campaign corresponds with relatively high CO and O_3 values, and also higher aerosol number concentrations. The cooling after day 20 is accompanied by a marked reduction in n_{CCN}, and also an increase in the fraction of aerosol which are activated to form cloud droplets. As can be seen in the bottom panel of each plot, the updraught

ACPD
15, 15469–15510, 2015

velocities are generally lower when the wind is from the southeast than when it is from the northwest, consistent with the findings of (Hammer et al., 2014a).

5.1 Statistical relationships for combined data

The modelled number of cloud droplets is plotted against the observed number (n_{act}), for a variety of model formulations, in Fig. (5). In panel a, only n_{CCN} is used to predict the number of cloud droplets. Already here a good relationship is found, with a correlation (R) of 0.87, however the intercept in the model leads to an unphysical cut off at low modelled numbers. Including the updraught velocity improves the model slightly, while the R value remains the same, the root mean squared error (RMSE) reduces slightly from 64.7 to 63.2. Further small improvements are found by including all the variables, and, in panel d, by using all variables as well as the log of the updraught velocity rather than the updraught velocity itself. This model was found to be the best representation of the observed number of droplets, with an R value of 0.88, RMSE of 60.6 and a mean error (ME) of 41.2.

The model presented in panel d of Fig. 5 provides a simple and reasonably accurate way of predicting the number of cloud droplets formed based on only a few explanatory variables. The number of activated aerosol (considered equivalent to the number of droplets) predicted by this model is given by:

$$n_{act} = 0.61 n_{CCN} + 2.12 O_3 + 0.04 H - 0.58 CO + 26.63 \log(\omega) - 57.38, \quad (2)$$

where ω is the estimated updraught velocity at cloud base in $m\,s^{-1}$, CO and O_3 are mixing ratios in ppb, and H is the height of the JFJ above the cloud base in meters (H must be greater than zero).

The model considering only the number of CCN, as shown in panel a of Fig. 5, is:

$$n_{act} = 0.62 n_{CCN} + 46.89 \quad (3)$$

The same analysis was performed with reductions in the minimum size of aerosol considered to be CCN to 80 and 70 nm (not shown), however this did not improve the

ACPD
15, 15469–15510, 2015

model in relation to the results obtained when counting only aerosol larger than 90 nm to determine n_{CCN}. It should be noted that at very low n_{CCN}, the model may return negative values for the number of droplets, which is obviously un-physical. However, this only applies to a very small number of points (16 of the 2399 points presented here), and thus does not compromise the general applicability of the proposed model.

5.2 Difference between wind directions

It was observed by Hammer et al. (2014a) that the number and properties of aerosol in air parcels approaching the JFJ from the southeast was slightly different from those in air approaching from the northwest. Further, they found that the activation diameter of particles differed between the two wind directions. Therefore the total data set used here was divided according to wind direction, and the model given by Eq. (2) was applied, to see if the model's ability to reproduce the observed number of droplets differed between the two wind directions. This comparison is plotted in Fig. 6. The R value for the north western wind direction (panel a) is larger than that for the south eastern wind direction (89 vs. 85), and the RMSE and ME are both substantially lower (RMSE of 53.2 vs. 79.8 and ME of 36.7 vs. 55.8). It can also be seen that most of the outlying points that the model underestimates at n_{CCN} greater than approximately 550 cm^{-3}, are in the south easterly wind data set. Additionally, the spread of points between 200 and 400 droplets is larger in the southeastern plot (panel b) than in the north western plot (panel a). In the northwesterly case it can be seen that the model shifts from a slight overestimation of the observed number of cloud droplets, to a slight underestimation, with the crossover occurring at about 150 drops cm^{-3}. On the other hand, the data in the south eastern case appears to follow the 1 : 1 line on average, at least up until about 500 drops cm^{-3} are reached. Therefore there appears to be no systematic bias introduced by considering both wind directions in the model together.

ACPD
15, 15469–15510, 2015

5.3 Difference between years

To determine how representative the model in Eq. (2) is for data from different years, the results were broken up into data for each year, shown in Fig. 7. For 2002, 2010 and 2011, the model provides a fairly compact correlation with the observed number of droplets, however the slope varies between different years. While the data from 2011 lies along the 1 : 1 line, the 2010 data seems to be composed of two different groups of points with different slopes, below and above approximately 300 drops cm^{-3}. It is not surprising that the R and error values are better for 2010 and 2011, as these years provide by far the most data points by which the model was fitted. The R for 2002 (0.95) was the highest of all years, however as the overall slope was lower than that for 2010 and 2011, most of the data points are below the 1 : 1 line and the RMSE was high (115.6). Further, it can be seen that most of the points which were underestimated by the model under south east wind conditions, at n_{act} greater than approximately 500 cm^{-3} (Fig. 6), come from 2002. The data collected during 2004 is not well fit by the model (R of 0.67, RMSE of 54.6). However, as there were so few data points in 2004, and these were mostly at low droplet numbers, it is difficult to say if this is due to the data sampled, or if the conditions were fundamentally different during 2004.

The differences between the years were also investigated by re-fitting the model to each individual year of data (Fig. 8). Naturally, this results in higher values of R, and smaller errors. For example, in 2002 a compact relationship is seen, with R of 0.96, and an RMSE of only 50.1. In this case, it can also be seen that the model underestimation of points above 500 drops cm^{-3} seen in previous plots is not due to a saturation effect, as the whole range of data for 2002 can be well represented with one set of parameters. The model representation of 2004 is improved when the model is tuned to only 2004 data, however the R value is still only 0.8, much lower than for the other years. This appears to be related to the overall low range of n_{CCN} observed in 2004. Both 2010 and 2011 are well represented by models tuned specifically to these data.

ACPD
15, 15469–15510, 2015

As a further way to assess the general applicability of the proposed linear model, 100 random data points (without replacement) were taken from each year of data, and the R and error values were calculated with (i) the general model and (ii) the models tuned to each sampled set of 400 observations (i.e., 100 observations from each year) separately. This analysis was performed 1000 times, and the results are summarised in Fig. 9. Due to the small number of data points in 2004 (210) and 2002 (206), the samples for these years did not differ greatly. In Fig. 9, it is apparent that the individually tuned models for the 1000 subsets perform slightly better than the simultaneously applied general model (as expected), however given the small differences in both R and error values between the individual and general models, illustrated by the overlap of the inner quartile ranges in both R and error values, the general model can be considered to be robust for the data set and applicable over a wide range of observed conditions.

6 Discussion

The analysis above shows that the number of cloud droplets can be reasonably well predicted by a single model, containing the n_{CCN}, the log of the updraught velocity, the height above cloud base and the mixing ratios of CO and O_3. The contribution of each variable to the variance explained by Eq. (2) is shown in Fig. 10, along with error bars, denoting the range of the contributions of each variable in the random sampling analysis described in the previous section. The range of the parameters included in Fig. 10 is relatively small, indicating that the contribution to the explained variance is similar regardless of the sample taken from the data set.

By far the greatest contribution to the explained variance is from n_{CCN}, however including additional explanatory variables does improve the model with respect to absolute biases. The lack of a strong dependence on updraught may be due to the method used to estimate the vertical wind speed, however as it is impractical to measure the actual wind speeds at the cloud base, this is the only method we have available. Fur-

ACPD
15, 15469–15510, 2015

ther, the fact that Hammer et al. (2014a) found that increasing the estimated updraught by a factor of four enabled a reasonable modelled reproduction of the peak supersaturations derived from measurements made during the CLACE2010 campaign would suggest that our estimated updraught is generally correlated with the updraught at cloud base, and therefore the use of it in the models developed here is justified.

The cloud base temperature was not found to be significantly correlated with the cloud droplet number over the combined data set suggesting that temperature dependent influences of surface active compounds do not play a significant role in cloud droplet activation. The O_3 and CO mixing ratios contributed around 10 and 4 % respectively of predictive ability to the model, suggesting that for sites such as the JFJ, which are located relatively far from direct emissions sources, the chemical history, or source region of the air mass is not greatly relevant in predicting the activation of aerosol to cloud droplets. Previously Jurányi et al. (2011) and Hammer et al. (2014a) have found that the hygroscopicity parameter of aerosols observed at the JFJ is not highly variable. The results presented here also indicate that changes in aerosol properties, which would generally be correlated with CO or O_3 concentrations, are not large enough to substantially influence aerosol activation.

The height above the cloud base, H, contributed a small amount (around 7 %) to the explained variance. This is likely due to the height above cloud base being a measure of the total amount of condensable water in the cloud, with greater condensable water generally leading to more droplets.

A previous study carried out at the JFJ, by Henning et al. (2002), found that when the number of potential CCN with diameter greater than 100 nm reduced below 100 cm^{-3}, the activation diameter shifted to smaller sizes, so that significant numbers of aerosol smaller than 100 nm began to activate. However, the ability of Eq. (2) to predict n_{act} does not deteriorate at low particle numbers, possibly because in this work, particles larger than 90 nm are considered potential CCN.

Finally, the general linear model presented in this study is compared with two existing parametrisations, those of Jones (1994) and Martin et al. (1994), both of which used

ACPD
15, 15469–15510, 2015

n_{CCN} to predict the number of cloud droplets which would be formed. The Martin et al. (1994) parametrisation is given by:

$$N_{droplets} = -2.10 \times 10^{-4} A^2 + 0.568A - 27.9 \quad (4)$$

where A is the number of aerosol in the size range 100 nm–3.0 µm in diameter. We use the version suggested for use in maritime air masses (their Eq. 12), as the version for continental air masses (their Eq. 13) produces a very poor representation of the number of observed droplets at the JFJ (not shown). This is possibly because the maritime parametrisation is more representative for air masses with relatively low aerosol number concentrations, as encountered at the JFJ. The maritime parametrisation is described as being valid over the range of aerosol number concentrations of 36 to 280 cm^{-3}.

The Jones (1994) parametrisation is derived from a combination of the continental and maritime parametrisations of Martin et al. (1994) and should therefore be valid over the range of aerosol number concentrations of 36 to 1500 cm^{-3}. It is given by:

$$N_{droplets} = 375(1 - \exp[-2.5 \times 10^{-3}\ A]) \quad (5)$$

The modelled cloud droplet number concentration is plotted against the measured values for Eqs. (2) and (3) as well as against the models of Martin et al. (1994) and Jones (1994), in Fig. 11. Comparison of Eqs. (2) and (3) with the other models considered shows that, although all four models provide a similar degree of explained variance (between 0.77 and 0.76), error values are vastly increased for the Jones (1994) and Martin et al. (1994) models. While all four models show a compact relationship between modelled and measured cloud droplet numbers, the model of Martin et al. (1994) has a too shallow slope, resulting in a general underestimation of the observed values. Both the Jones (1994) and Martin et al. (1994) models have included a saturation effect at higher n_{CCN} which limits the number of cloud droplets formed, similarly to the effect described by Reutter et al. (2009). No such saturation effect is observed at

ACPD
15, 15469–15510, 2015

the JFJ, however it cannot be ruled out that such an effect may occur at higher aerosol number concentrations than those presented here.

In Table 2, the Jones and the Martin model are compared with Eqs. (2) and (3) in terms of the fraction of data points which they predict within certain percentage limits of the observed n_{act}. The ability of the latter two equations to represent the observed droplet numbers is especially evident when comparing the number of modelled points within 10 or 20 % of the observed values. While Eqs. (2) and (3) are able to predict approximately 47 and 42 % of the data points to within 20 % of the observed n_{act} values, the Martin et al. (1994) and Jones (1994) models only place approximately 3 and 26 % of the points within these limits, respectively.

7 Conclusions

Using data from four summertime CLACE campaigns performed at the high altitude research station at the Jungfraujoch, we have shown that the number of cloud droplets formed in warm clouds can be rather accurately represented by a simple statistical model (Eq. 2). The majority of the variance in the observed droplet numbers is explained by the number of potential CCN, which is defined in this study as the total number of particles with a dry diameter greater than 90 nm. Using the number of CCN alone, 76 % of the observed variance is explained (Eq. 3). With the addition of further explanatory variables, such as CO and O_3 mixing ratios, and the height above cloud base, the RMSE and ME errors can be slightly reduced.

Although tuning the model to each year of data separately produces slightly improved results, Eq. (2) represents the observed droplet numbers from the individual years quite adequately. Likewise, the model is applicable to data from both of the predominant wind directions, and although there is more variability in the models ability to predict the number of droplets formed during southeasterly wind conditions, there appears to be no substantial bias.

ACPD
15, 15469–15510, 2015

In contrast to previous studies where such models were constructed (e.g. Martin et al., 1994; Jones, 1994), no evidence for a saturation effect of high CCN numbers was observed, rather the number of droplets formed increased continually with n_{CCN}. Although such a saturation effect may occur at higher aerosol number concentrations, such higher concentrations are likely to be relatively rare outside of the boundary layer.

Due to the location of the JFJ station predominantly in the free troposphere, on the alpine divide, with air masses approaching from both the north and the south, we expect Eqs. (2) and (3) to be broadly applicable to the European free troposphere. While such empirically derived relationships have their limitations, and may not remain valid under substantially perturbed atmospheric conditions, they provide a simple and computationally efficient way to calculate the number of cloud droplets in warm clouds.

Acknowledgements. C. R. Hoyle was funded by Swiss National Science Foundation (SNSF) grant number 200021_140663. M. Gysel was supported by the ERC under grant 615922-BLACARAT. EU FP7 project BACCHUS (project number 603445) is acknowledged for financial support. The CLACE experiments were supported by the Global Atmosphere Watch plus (GAW+) research program. Meteorological measurements from the SwissMetNet Network were obtained through Meteoswiss. The JFJ experimental site is supported by the International Foundation High Altitude Research Stations Jungfraujoch and Gornergrat (HFSJG). The Swiss National Air Pollution Monitoring Network is run by Empa in collaboration with the Swiss Federal Office for the Environment.

References

Albrecht, B. A.: Aerosols, cloud microphysics, and fractional cloudiness, Science, 245, 1227–1230, doi:10.1126/science.245.4923.1227, 1989. 15471

Anttila, T., Brus, D., Jaatinen, A., Hyvärinen, A.-P., Kivekäs, N., Romakkaniemi, S., Komppula, M., and Lihavainen, H.: Relationships between particles, cloud condensation nuclei and cloud droplet activation during the third Pallas Cloud Experiment, Atmos. Chem. Phys., 12, 11435–11450, doi:10.5194/acp-12-11435-2012, 2012. 15472

ACPD
15, 15469–15510, 2015

Baltensperger, U., Gaggeler, H., Jost, D., Emmenegger, M., and Nageli, W.: Continuous background aerosol monitoring wiht the epiphaniometer, Atmos. Environ. A-Gen., 25, 629–634, doi:10.1016/0960-1686(91)90060-K, 1991. 15474

Baltensperger, U., Gaggeler, H. W., Jost, D. T., Lugauer, M., Schwikowski, M., Weingartner, E., and Seibert, P.: Aerosol climatology at the high-alpine site Jungfraujoch, Switzerland, J. Geophys. Res.-Atmos., 102, 19707–19715, doi:10.1029/97jd00928, 1997. 15474

Baltensperger, U., Schwikowski, M., Jost, D. T., Nyeki, S., Gaggeler, H. W., and Poulida, O.: Scavenging of atmospheric constituents in mixed phase clouds at the high-alpine site Jungfraujoch part I: Basic concept and aerosol scavenging by clouds, Atmos. Environ., 32, 3975–3983, doi:10.1016/S1352-2310(98)00051-X, 1998. 15474

Barahona, D. and Nenes, A.: Parameterization of cloud droplet formation in large-scale models: including effects of entrainment, J. Geophys. Res.-Atmos., 112, D16206, doi:10.1029/2007JD008473, 2007. 15472

Boucher, O., Randall, D., Artaxo, P., Bretherton, C., Feingold, G., Forster, P., Kerminen, V.-M., Kondo, Y., Liao, H., Lohmann, U., Rasch, P., Satheesh, S., Sherwood, S., Stevens, B., and Zhang, X.: Cloud and aerosols, in: Climate Change 2013: The Physical Science Basis. Contribution of Working Group I to the Fifth Assessment Report of the Intergovernmental Panel on Climate Change, edited by: Stocker, T. F., Qin, D., Plattner, G.-K., Tignor, M., Allen, S. K., Boschung, J., Nauels, A., Xia, Y., Bex, V., and Midgley, P. M., Cambridge University Press, Cambridge, UK and New York, NY, USA, 571–657, 2013. 15471

Christensen, S. I. and Petters, M. D.: The role of temperature in cloud droplet activation, J. Phys. Chem. A, 116, 9706–9717, doi:10.1021/jp3064454, 2012. 15473

Cozic, J., Verheggen, B., Mertes, S., Connolly, P., Bower, K., Petzold, A., Baltensperger, U., and Weingartner, E.: Scavenging of black carbon in mixed phase clouds at the high alpine site Jungfraujoch, Atmos. Chem. Phys., 7, 1797–1807, doi:10.5194/acp-7-1797-2007, 2007. 15498

Cozic, J., Verheggen, B., Weingartner, E., Crosier, J., Bower, K. N., Flynn, M., Coe, H., Henning, S., Steinbacher, M., Henne, S., Collaud Coen, M., Petzold, A., and Baltensperger, U.: Chemical composition of free tropospheric aerosol for PM1 and coarse mode at the high alpine site Jungfraujoch, Atmos. Chem. Phys., 8, 407–423, doi:10.5194/acp-8-407-2008, 2008. 15479

Cui, J., Sprenger, M., Staehelin, J., Siegrist, A., Kunz, M., Henne, S., and Steinbacher, M.: Impact of stratospheric intrusions and intercontinental transport on ozone at Jungfraujoch

ACPD
15, 15469–15510, 2015

in 2005: comparison and validation of two Lagrangian approaches, Atmos. Chem. Phys., 9, 3371–3383, doi:10.5194/acp-9-3371-2009, 2009. 15481
Dusek, U., Frank, G. P., Hildebrandt, L., Curtius, J., Schneider, J., Walter, S., Chand, D., Drewnick, F., Hings, S., Jung, D., Borrmann, S., and Andreae, M. O.: Size Mmatters more than chemistry for cloud-nucleating ability of aerosol particles, Science, 312, 1375–1378, doi:10.1126/science.1125261, 2006. 15472, 15473
Fitzgerald, J. W. and Spyers-Duran, P. A.: Changes in cloud nucleus concentration and cloud droplet size distribution associated with pollution from St. Louis, J. Appl. Meteorol., 12, 511–516, doi:10.1175/1520-0450(1973)012<0511:CICNCA>2.0.CO;2, 1973. 15472
Fountoukis, C. and Nenes, A.: Continued development of a cloud droplet formation parameterization for global climate models, J. Geophys. Res.-Atmos., 110, D11212, doi:10.1029/2004JD005591, 2005. 15472
Gerber, H.: Supersaturation and droplet spectral evolution in fog, J. Atmos. Sci., 48, 2569–2588, doi:10.1175/1520-0469(1991)048<2569:SADSEI>2.0.CO;2, 1991. 15477
Gilge, S., Plass-Duelmer, C., Fricke, W., Kaiser, A., Ries, L., Buchmann, B., and Steinbacher, M.: Ozone, carbon monoxide and nitrogen oxides time series at four alpine GAW mountain stations in central Europe, Atmos. Chem. Phys., 10, 12295–12316, doi:10.5194/acp-10-12295-2010, 2010. 15478, 15481
Grömping, U.: Relative importance for linear regression in *R*: the package relaimpo, J. Stat. Softw., 17, 1–27, 2006. 15482
Grömping, U.: Estimators of relative importance in linear regression based on variance decomposition, Am. Stat., 61, 139–147, doi:10.1198/000313007X188252, 2007. 15482
Hammer, E., Bukowiecki, N., Gysel, M., Jurányi, Z., Hoyle, C. R., Vogt, R., Baltensperger, U., and Weingartner, E.: Investigation of the effective peak supersaturation for liquid-phase clouds at the high-alpine site Jungfraujoch, Switzerland (3580 m a.s.l.), Atmos. Chem. Phys., 14, 1123–1139, doi:10.5194/acp-14-1123-2014, 2014a. 15475, 15476, 15477, 15479, 15480, 15481, 15484, 15485, 15488, 15498
Hammer, E., Bukowiecki, N., Luo, B. P., Lohmann, U., Marcolli, C., Weingartner, E., Baltensperger, U., and Hoyle, C. R.: Sensitivity estimations for cloud droplet formation in the vicinity of the high alpine research station Jungfraujoch (3580 m a.s.l.), Atmos. Chem. Phys. Discuss., 14, 25967–26002, doi:10.5194/acpd-14-25967-2014, 2014b. 15475
Henning, S., Weingartner, E., Schmidt, S., Wendisch, M., Gaggeler, H. W., and Baltensperger, U.: Size-dependent aerosol activation at the high-alpine site Jungfraujoch

ACPD
15, 15469–15510, 2015

(3580 m asl), Tellus B, 54, 82–95, doi:10.1034/j.1600-0889.2002.00299.x, 2002. 15472, 15473, 15475, 15476, 15479, 15481, 15488
Hu, Y. X. and Stamnes, K.: An accurate parameterization of the radiative properties of water clouds suitable for use in climate models, J. Climate, 6, 728–742, doi:10.1175/1520-0442(1993)006<0728:AAPOTR>2.0.CO;2, 1993. 15471
Johnson, B. T., Shine, K. P., and Forster, P. M.: The semi-direct aerosol effect: Impact of absorbing aerosols on marine stratocumulus, Q. J. Roy. Meteor. Soc., 130, 1407–1422, doi:10.1256/qj.03.61, 2004. 15482
Jones, A.: A climate model study of indirect radiative forcing by anthropogenic sulphate aerosols, Nature, 370, 450–453, 1994. 15472, 15488, 15489, 15490, 15491, 15510
Jurányi, Z., Gysel, M., Weingartner, E., DeCarlo, P. F., Kammermann, L., and Baltensperger, U.: Measured and modelled cloud condensation nuclei number concentration at the high alpine site Jungfraujoch, Atmos. Chem. Phys., 10, 7891–7906, doi:10.5194/acp-10-7891-2010, 2010. 15472, 15473, 15476
Jurányi, Z., Gysel, M., Weingartner, E., Bukowiecki, N., Kammermann, L., and Baltensperger, U.: A 17 month climatology of the cloud condensation nuclei number concentration at the high alpine site Jungfraujoch, J. Geophys. Res.-Atmos., 116, 2156–2202, doi:10.1029/2010JD015199, 2011. 15472, 15473, 15476, 15488
Kammermann, L., Gysel, M., Weingartner, E., and Baltensperger, U.: 13-month climatology of the aerosol hygroscopicity at the free tropospheric site Jungfraujoch (3580 m a.s.l.), Atmos. Chem. Phys., 10, 10717–10732, doi:10.5194/acp-10-10717-2010, 2010. 15476
King, S. M., Rosenoern, T., Shilling, J. E., Chen, Q., and Martin, S. T.: Increased cloud activation potential of secondary organic aerosol for atmospheric mass loadings, Atmos. Chem. Phys., 9, 2959–2971, doi:10.5194/acp-9-2959-2009, 2009. 15473
Köhler, H.: The nucleus in and the growth of hygroscopic droplets, T. Faraday Soc., 32, 1152–1161, doi:10.1039/TF9363201152, 1936. 15472, 15473
Kruskal, W.: Relative importance by averaging over orderings, Am. Stat., 41, 6–10, doi:10.2307/2684310, 1987. 15482
Kumar, P., Sokolik, I. N., and Nenes, A.: Parameterization of cloud droplet formation for global and regional models: including adsorption activation from insoluble CCN, Atmos. Chem. Phys., 9, 2517–2532, doi:10.5194/acp-9-2517-2009, 2009. 15472
Liang, Q., Jaegle, L., Jaffe, D., Weiss-Penzias, P., Heckman, A., and Snow, J.: Long-range transport of Asian pollution to the northeast Pacific: seasonal variations and transport pathways

ACPD
15, 15469–15510, 2015

of carbon monoxide, J. Geophys. Res.-Atmos., 109, D23S07, doi:10.1029/2003JD004402, 2004. 15481
Lindeman, R. H., Merenda, P. F., and Gold, R.: Introduction to Bivariate and Multivariate Analysis, Scott Foresman, Glenview, IL, 1980. 15482
Lugauer, M., Baltensperger, U., Furger, M., Gaggeler, H., Jost, D., Schwikowski, M., and Wanner, H.: Aerosol transport to the high Alpine sites Jungfraujoch (3454 m asl) and Colle Gnifetti (4452 m asl), Tellus B, 50, 76–92, doi:10.1034/j.1600-0889.1998.00006.x, 1998. 15475
Martin, G. M., Johnson, D. W., and Spice, A.: The measurement and parameterization of effective radius of droplets in warm stratocumulus clouds, J. Atmos. Sci., 51, 1823–1842, doi:10.1175/1520-0469(1994)051<1823:TMAPOE>2.0.CO;2, 1994. 15472, 15488, 15489, 15490, 15491, 15510
McFiggans, G., Artaxo, P., Baltensperger, U., Coe, H., Facchini, M. C., Feingold, G., Fuzzi, S., Gysel, M., Laaksonen, A., Lohmann, U., Mentel, T. F., Murphy, D. M., O'Dowd, C. D., Snider, J. R., and Weingartner, E.: The effect of physical and chemical aerosol properties on warm cloud droplet activation, Atmos. Chem. Phys., 6, 2593–2649, doi:10.5194/acp-6-2593-2006, 2006. 15473
Nenes, A. and Seinfeld, J. H.: Parameterization of cloud droplet formation in global climate models, J. Geophys. Res.-Atmos., 108, 4415, doi:10.1029/2002JD002911, 2003. 15472
Nyeki, S., Li, F., Weingartner, E., Streit, N., Colbeck, I., Gaggeler, H. W., and Baltensperger, U.: The background aerosol size distribution in the free troposphere: an analysis of the annual cycle at a high-alpine site, J. Geophys. Res.-Atmos., 103, 31749–31761, doi:10.1029/1998jd200029, 1998. 15474, 15475
Petters, M. D. and Kreidenweis, S. M.: A single parameter representation of hygroscopic growth and cloud condensation nucleus activity, Atmos. Chem. Phys., 7, 1961–1971, doi:10.5194/acp-7-1961-2007, 2007. 15472, 15473
R Core Team: R: A Language and Environment for Statistical Computing, R Foundation for Statistical Computing, Vienna, Austria, available at: http://www.R-project.org (last access: 9 June 2015), ISBN 3-900051-07-0, 2014. 15482
Raga, G. B. and Jonas, P. R.: On the link between cloud-top radiative properties and sub-cloud aerosol concentrations, Q. J. Roy. Meteor. Soc., 119, 1419–1425, doi:10.1002/qj.49711951410, 1993. 15472
Reutter, P., Su, H., Trentmann, J., Simmel, M., Rose, D., Gunthe, S. S., Wernli, H., Andreae, M. O., and Pöschl, U.: Aerosol- and updraft-limited regimes of cloud droplet formation:

ACPD
15, 15469–15510, 2015

influence of particle number, size and hygroscopicity on the activation of cloud condensation nuclei (CCN), Atmos. Chem. Phys., 9, 7067–7080, doi:10.5194/acp-9-7067-2009, 2009. 15473, 15489

Shilling, J. E., King, S. M., Mochida, M., and Martin, S. T.: Mass spectral evidence that small changes in composition caused by oxidative aging processes alter aerosol CCN properties, J. Phys. Chem. A, 111, 3358–3368, doi:10.1021/jp068822r, 2007. 15473

Shulman, M., Jacobson, M., Carlson, R., Synovec, R., and Young, T.: Dissolution behavior and surface tension effects of organic compounds in nucleating cloud droplets, Geophys. Res. Lett., 23, 277–280, doi:10.1029/95GL03810, 1996. 15473

Sjogren, S., Gysel, M., Weingartner, E., Alfarra, M. R., Duplissy, J., Cozic, J., Crosier, J., Coe, H., and Baltensperger, U.: Hygroscopicity of the submicrometer aerosol at the high-alpine site Jungfraujoch, 3580 m a.s.l., Switzerland, Atmos. Chem. Phys., 8, 5715–5729, doi:10.5194/acp-8-5715-2008, 2008. 15475

Spiegel, J. K., Zieger, P., Bukowiecki, N., Hammer, E., Weingartner, E., and Eugster, W.: Evaluating the capabilities and uncertainties of droplet measurements for the fog droplet spectrometer (FM-100), Atmos. Meas. Tech., 5, 2237–2260, doi:10.5194/amt-5-2237-2012, 2012. 15498

Staudt, A., Jacob, D., Logan, J., Bachiochi, D., Krishnamurti, T., and Sachse, G.: Continental sources, transoceanic transport, and interhemispheric exchange of carbon monoxide over the Pacific, J. Geophys. Res.-Atmos., 106, 32571–32589, doi:10.1029/2001JD900078, 2001. 15481

Tonidandel, S. and LeBreton, J. M.: Relative importance analysis: a useful supplement to regression analysis, J. Bus. Psychol., 26, 1–9, doi:10.1007/s10869-010-9204-3, 2011. 15482

Twomey, S.: Pollution and the planetary albedo, Atmos. Environ., 8, 1251–1256, doi:10.1016/0004-6981(74)90004-3, 1974. 15471, 15472

Twomey, S. A.: The influence of pollution on the shortwave albedo of clouds, J. Atmos. Sci., 34, 1149–1152, doi:10.1175/1520-0469(1977)034<1149:TIOPOT>2.0.CO;2, 1977. 15471, 15472

Verheggen, B., Cozic, J., Weingartner, E., Bower, K., Mertes, S., Connolly, P., Gallagher, M., Flynn, M., Choularton, T., and Baltensperger, U.: Aerosol partitioning between the interstitial and the condensed phase in mixed-phase clouds, J. Geophys. Res.-Atmos., 112, 2156–2202, doi:10.1029/2007JD008714, 2007. 15472, 15473, 15475, 15477

ACPD
15, 15469–15510, 2015

Weingartner, E., Nyeki, S., and Baltensperger, U.: Seasonal and diurnal variation of aerosol size distributions (10 D 750 nm) at a high-alpine site (Jungfraujoch 3580 m asl), J. Geophys. Res.-Atmos., 104, 26809–26820, 1999. 15476

Wiedensohler, A., Birmili, W., Nowak, A., Sonntag, A., Weinhold, K., Merkel, M., Wehner, B., Tuch, T., Pfeifer, S., Fiebig, M., Fjäraa, A. M., Asmi, E., Sellegri, K., Depuy, R., Venzac, H., Villani, P., Laj, P., Aalto, P., Ogren, J. A., Swietlicki, E., Williams, P., Roldin, P., Quincey, P., Hüglin, C., Fierz-Schmidhauser, R., Gysel, M., Weingartner, E., Riccobono, F., Santos, S., Grüning, C., Faloon, K., Beddows, D., Harrison, R., Monahan, C., Jennings, S. G., O'Dowd, C. D., Marinoni, A., Horn, H.-G., Keck, L., Jiang, J., Scheckman, J., McMurry, P. H., Deng, Z., Zhao, C. S., Moerman, M., Henzing, B., de Leeuw, G., Löschau, G., and Bastian, S.: Mobility particle size spectrometers: harmonization of technical standards and data structure to facilitate high quality long-term observations of atmospheric particle number size distributions, Atmos. Meas. Tech., 5, 657–685, doi:10.5194/amt-5-657-2012, 2012. 15477

Yashiro, H., Sugawara, S., Sudo, K., Aoki, S., and Nakazawa, T.: Temporal and spatial variations of carbon monoxide over the western part of the Pacific Ocean, J. Geophys. Res.-Atmos., 114, D08305, doi:10.1029/2008JD010876, 2009. 15481

Zellweger, C., Forrer, J., Hofer, P., Nyeki, S., Schwarzenbach, B., Weingartner, E., Ammann, M., and Baltensperger, U.: Partitioning of reactive nitrogen (NO_y) and dependence on meteorological conditions in the lower free troposphere, Atmos. Chem. Phys., 3, 779–796, doi:10.5194/acp-3-779-2003, 2003. 15475

Zellweger, C., Hüglin, C., Klausen, J., Steinbacher, M., Vollmer, M., and Buchmann, B.: Intercomparison of four different carbon monoxide measurement techniques and evaluation of the long-term carbon monoxide time series of Jungfraujoch, Atmos. Chem. Phys., 9, 3491–3503, doi:10.5194/acp-9-3491-2009, 2009. 15478

Zhang, L., Jacob, D. J., Bowman, K. W., Logan, J. A., Turquety, S., Hudman, R. C., Li, Q., Beer, R., Worden, H. M., Worden, J. R., Rinsland, C. P., Kulawik, S. S., Lampel, M. C., Shephard, M. W., Fisher, B. M., Eldering, A., and Avery, M. A.: Ozone-CO correlations determined by the TES satellite instrument in continental outflow regions, Geophys. Res. Lett., 33, L18804, doi:10.1029/2006GL026399, 2006. 15481

Zhang, L., Jacob, D. J., Kopacz, M., Henze, D. K., Singh, K., and Jaffe, D. A.: Intercontinental source attribution of ozone pollution at western US sites using an adjoint method, Geophys. Res. Lett., 36, L18804, doi:10.1029/2006GL026399, 2009. 15481

ACPD
15, 15469–15510, 2015

Table 1. Dates and references for each CLACE campaign.

Campaign	Start date	End date	Reference
CLACE2002	4 Jul 2002	20 Jul 2002	–
CLACE2004	16 Jul 2004	30 Sep 2004	Cozic et al. (2007)
CLACE2010	1 Jul 2010	13 Aug 2010	Spiegel et al. (2012)
CLACE2011	1 Jul 2011	23 Aug2011	Hammer et al. (2014a)

ACPD
15, 15469–15510, 2015

Table 2. The percentage of model predicted droplet numbers within particular percentage limits of the observed values for each of the models considered.

Model	10 %	20 %	50 %
Eq. (2)	24.3	46.5	74.1
Eq. (3)	23.1	41.7	72.5
Martin	1.5	3.4	21.8
Jones	10.7	26.1	71.7

ACPD
15, 15469–15510, 2015

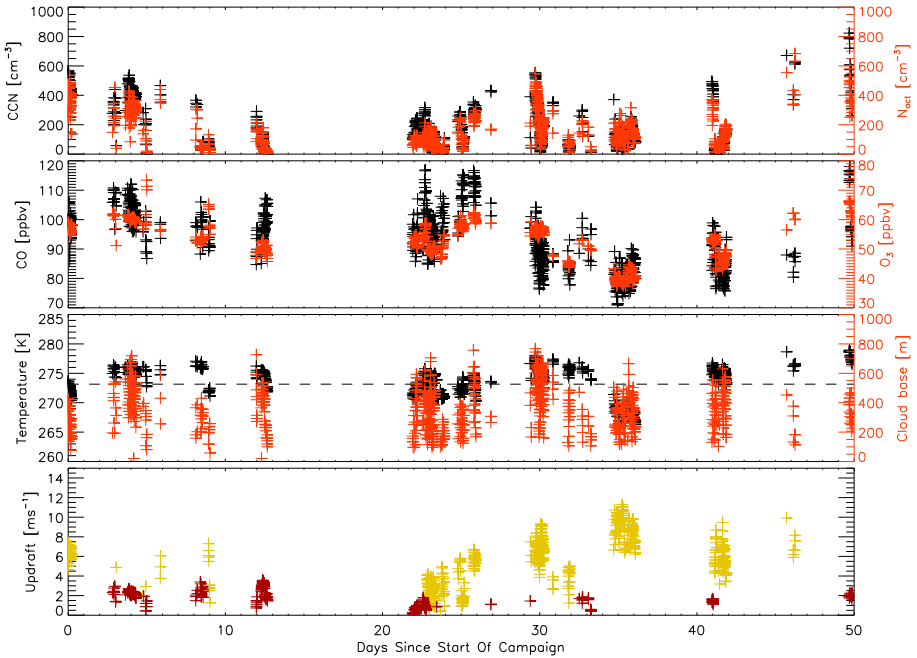

Figure 1. Time series for several quantities measured directly during the CLACE2011 campaign, or derived from other CLACE2011 data. The number of CCN, shown in the top panel, refers the number of particles larger than 90 nm in diameter, which are considered potential CCN in constructing the statistical models (see text). In the bottom panel, the colour of the points indicates the wind direction, with yellow showing wind classified as being northwest and red southeast. Data are only plotted for times when the JFJ was in-cloud.

ACPD
15, 15469–15510, 2015

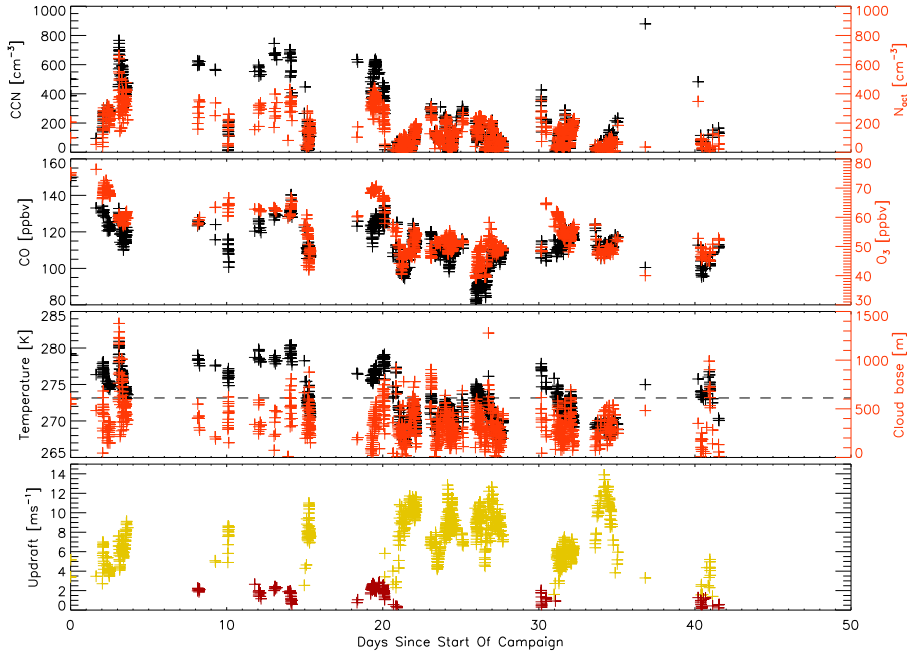

Figure 2. As for Fig. 1, but for CLACE2010. Note that the axis ranges differ from those in Fig. 1.

ACPD
15, 15469–15510, 2015

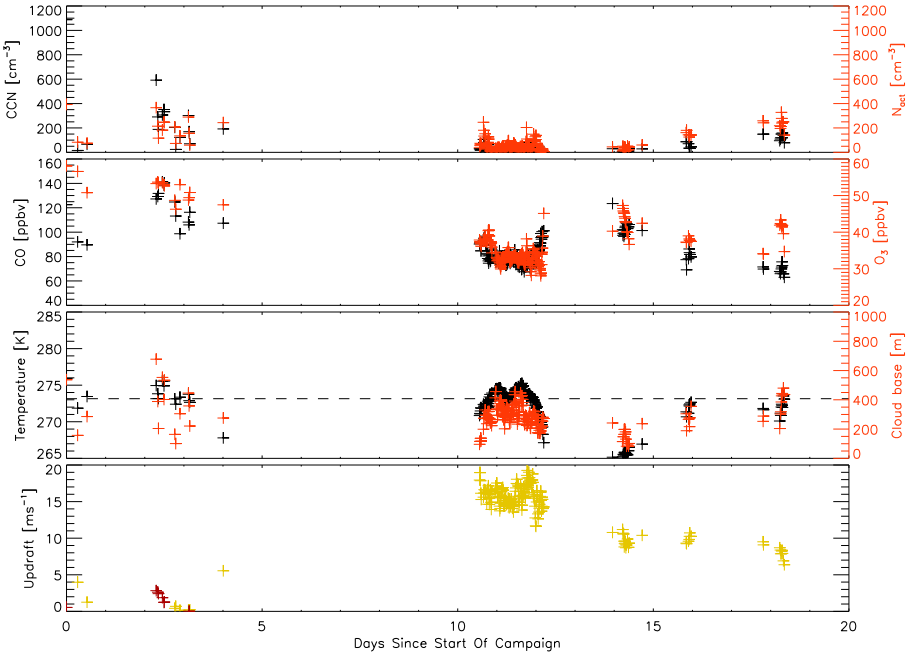

Figure 3. As for Fig. 1, but for CLACE2004. Note that the axis ranges differ from those in Fig. 1.

ACPD
15, 15469–15510, 2015

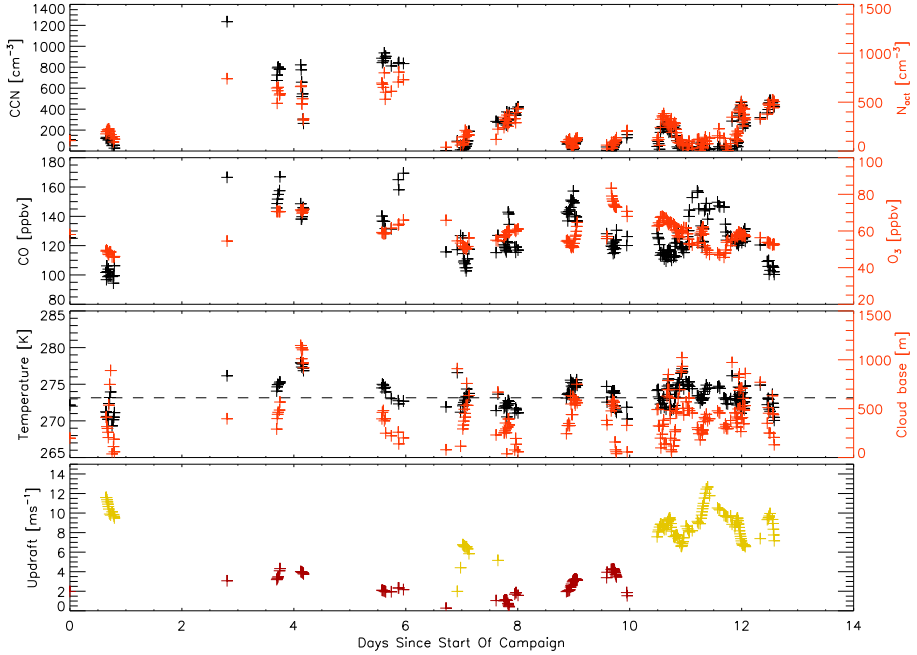

Figure 4. As for Fig. 1, but for CLACE2002. Note that the axis ranges differ from those in Fig. 1.

ACPD
15, 15469–15510, 2015

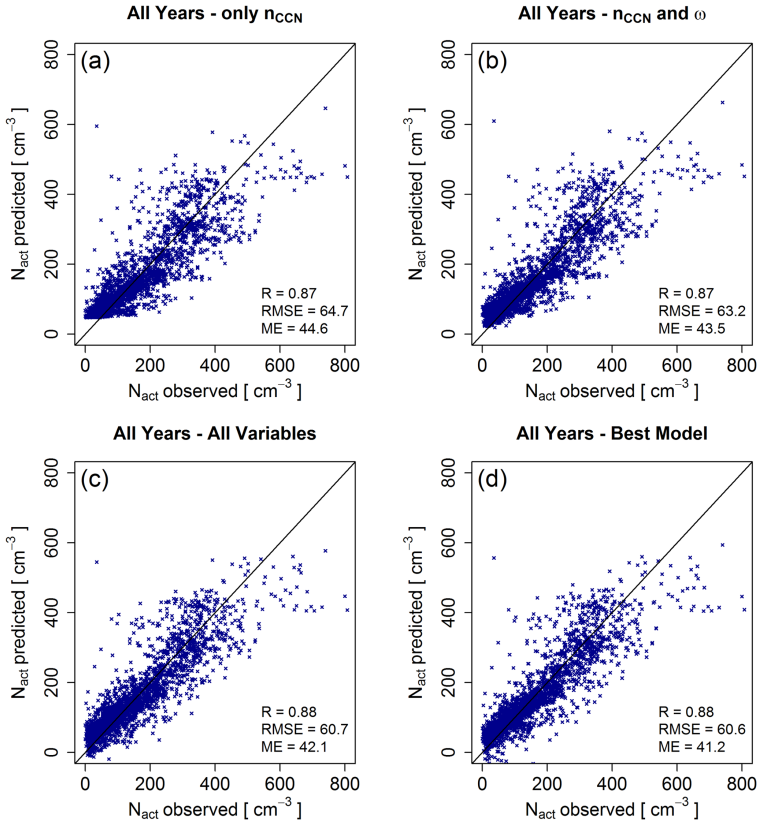

Figure 5. The modelled number of cloud droplets plotted against the observed number of residuals. The model used for panel **(a)** included only the n_{CCN}, for **(b)** n_{CCN} and updraught velocity are included in the model, and in panel **(c)** all variables are included. In panel **(d)**, all variables are included, however the log of the updraught velocity is used.

ACPD
15, 15469–15510, 2015

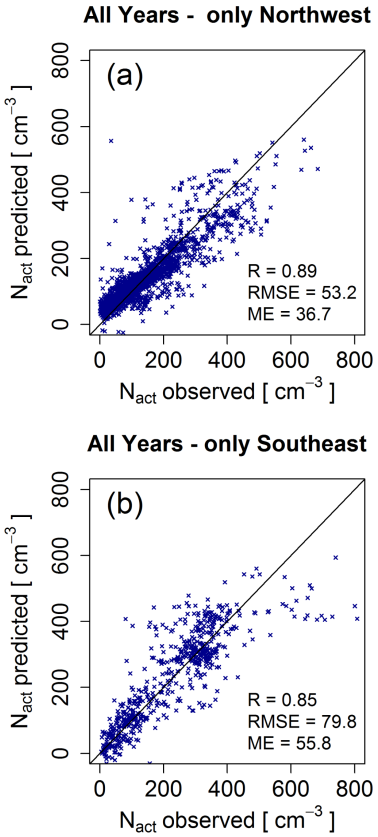

Figure 6. The modelled number of cloud droplets (Eq. 2) plotted against the observed number of residuals. Only data for north western wind conditions are included in panel **(a)**, while only data for south eastern wind directions are included in panel **(b)**.

ACPD
15, 15469–15510, 2015

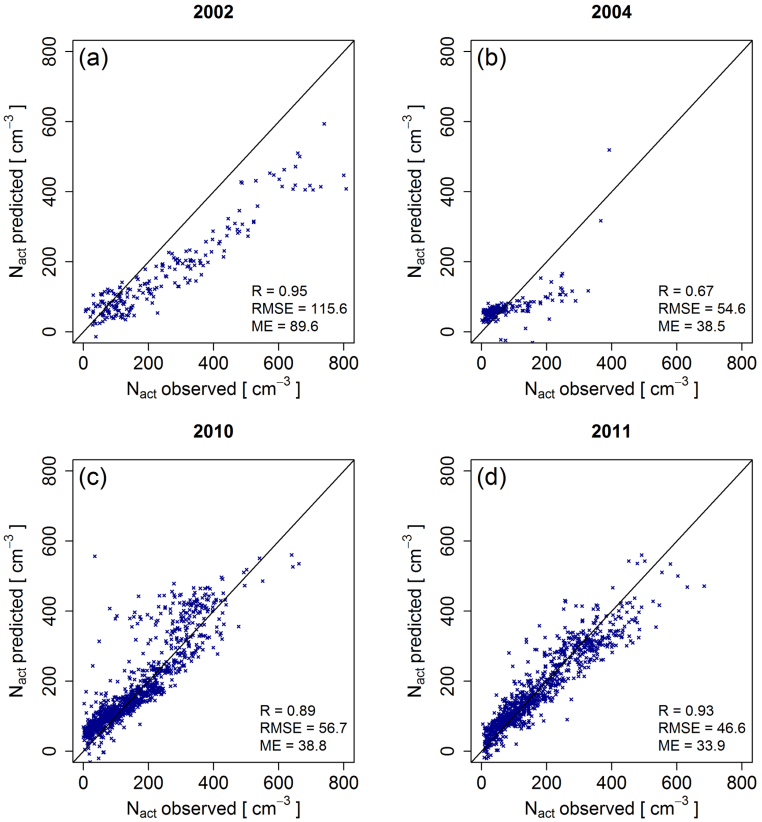

Figure 7. The modelled droplet numbers (Eq. 2) plotted against the observed number of residuals for each year separately.

ACPD
15, 15469–15510, 2015

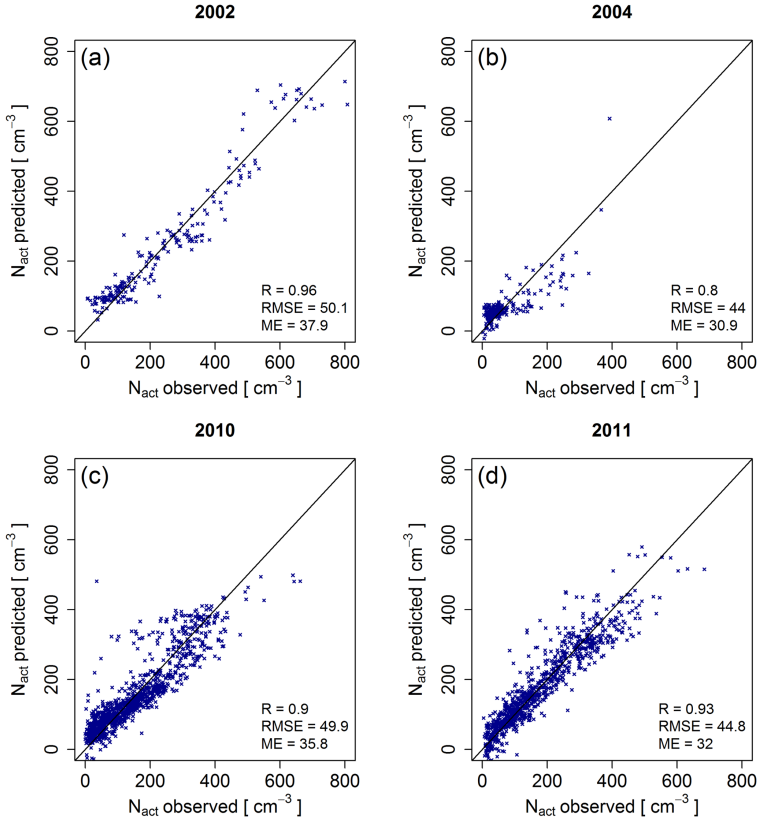

Figure 8. As for Fig. 7, however the model was re-calculated to provide the best fit for each year individually.

ACPD
15, 15469–15510, 2015

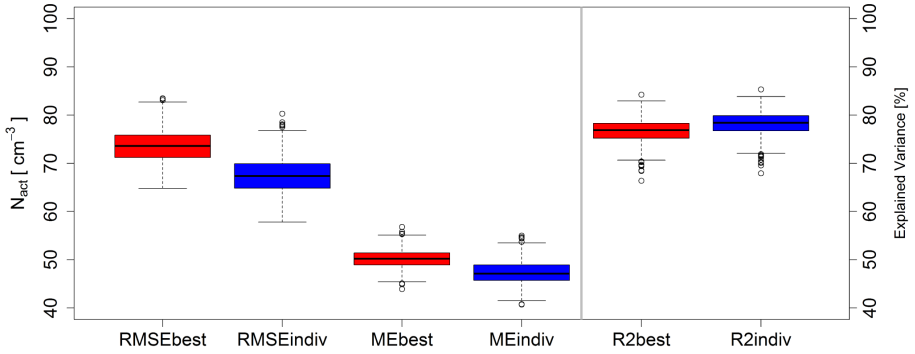

Figure 9. A box plot of the R^2, RMSE and ME values for the application of the general model (Eq. 2) to 1000 random samples of 100 data points from each year.

ACPD
15, 15469–15510, 2015

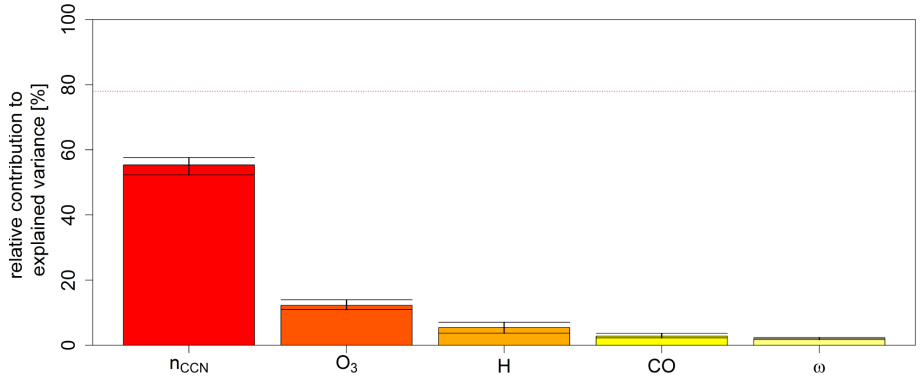

Figure 10. The contribution of each of the model variables in Eq. (2) to the explained variance. The error bars show the spread of the variation of the contribution values in the random samples from Fig. 9.

ACPD
15, 15469–15510, 2015

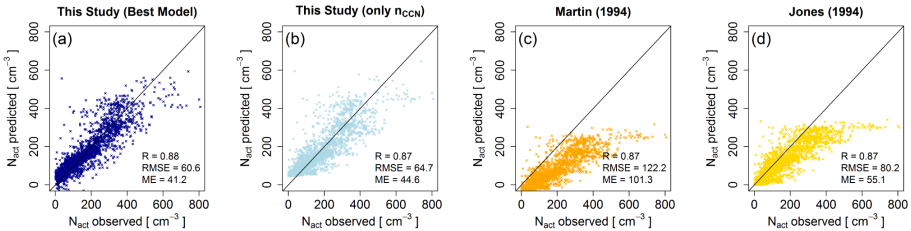

Figure 11. A comparison of the model developed in this study with the performance of two existing models, those of Martin et al. (1994) and Jones (1994), which are based only on n_{CCN}.

ACPD
15, 15469–15510, 2015